CLIMATE PATTERN RECOGNITION IN THE LATE-TO-END HOLOCENE (550 AD TO 1650 AD, PART 7)

JOACHIM SEIFERT

FRANK LEMKE

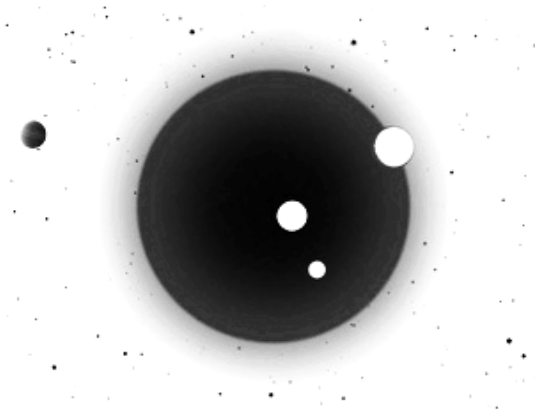

Correspondence to: weltklima@googlemail.com

Website: http://www.knowledgeminer.eu • http://www.climateprediction.eu

JUNE 2017

©2017 Joachim Seifert

Abstract. This 1,100 year time span, 550-1650 AD, consists of four distinct climate pattern periods. Each period shows the prevalence of only one of five existing cosmic climate driving mechanisms. The first distinct period is 550-1050 AD, consisting of a large double spike cosmic meteor impact pattern. The background is that each meteor impact of size leaves this particular pattern imprint within the entire GISP2 time series. The double spike consists of one cold spike at first, to 744 AD, also termed Late Antique Little Ice Age (LALIA), then followed by the second half of this pattern, the warm spike, to 985 AD, the Medieval Warm Period (MWP). This pattern ends after 500 years in 1050 AD. Thereafter, the second pattern sets in: Two clean 62 year Solar Inertial Movement (SIM) patterns in a row; the pattern is generally known by its effect on ocean heating and cooling, as AMO and PDO cycles. Two distinct warm SIM cycle peaks appear in GISP2. The robustness of the 62 year cycle length can be verified by backtracking this exact cycle length over multi-millennia, over more than 100 cycles in line, in the Holocene. The third pattern period starts in 1178 AD, and is caused by a strong cosmic lunar meteor impact. At this date, this impact displaced the Earth-Moon Barycenter (EMB), which then spirals back in 4 complete loops onto its regular EMB flight path around the Sun, for the following 400 years. This steady continuous closing in by four spiral loops onto the normal EMB orbital flight path around the Sun is clearly visible in the GISP2 data between 1207 AD and 1590 AD. The fourth pattern period is the EOO (Earth Orbit Oscillation) with its low temperature trough, 1590-1640 AD, which marks the very bottom of the Little Ice Age (LIA), with a minimum trough temperature of -32.08°C on the GISP2 borehole temperature scale. This minimum trough marks the end of the 29th half-wave Earth Orbital Oscillation (EOO) period, 432 years in length. Those orbital oscillations are growing cycles; they commenced in 8108 BC, with an initial half-wave length of 238 years, growing in succession by 6.93 years per half-wave. Out of the EOO-LIA minimum temperature trough, temperatures are bound to rise for 439 years, to the top of the 30th half-wave, which is the next high temperature peak, in 2049 AD. Details will be given in the part 8 paper, soon to follow.

Citation. Seifert, J., Lemke, F.: Climate pattern recognition in the late-to-end Holocene (550 AD to 1650 AD, part 7), 2017, http://www.knowledgeminer.eu/climate_papers.html

1. APPLICATION OF THE PATTERN RECOGNITION GRID

In figure 1, the GISP2 temperature time series (Alley, 2000, 2004), transformed into equidistant time steps, and the selected time span of this paper is shown.

As in all previous papers, we placed our standard pattern recognition grid onto the analyzed time span. Please refer to figure 2 of the Holocene part 6 analysis, showing a larger time span, 2000 BC to 2000 AD. From this figure 2, we use the second half, 1 AD to 2000 AD. Explanation: The first step of placing the pattern

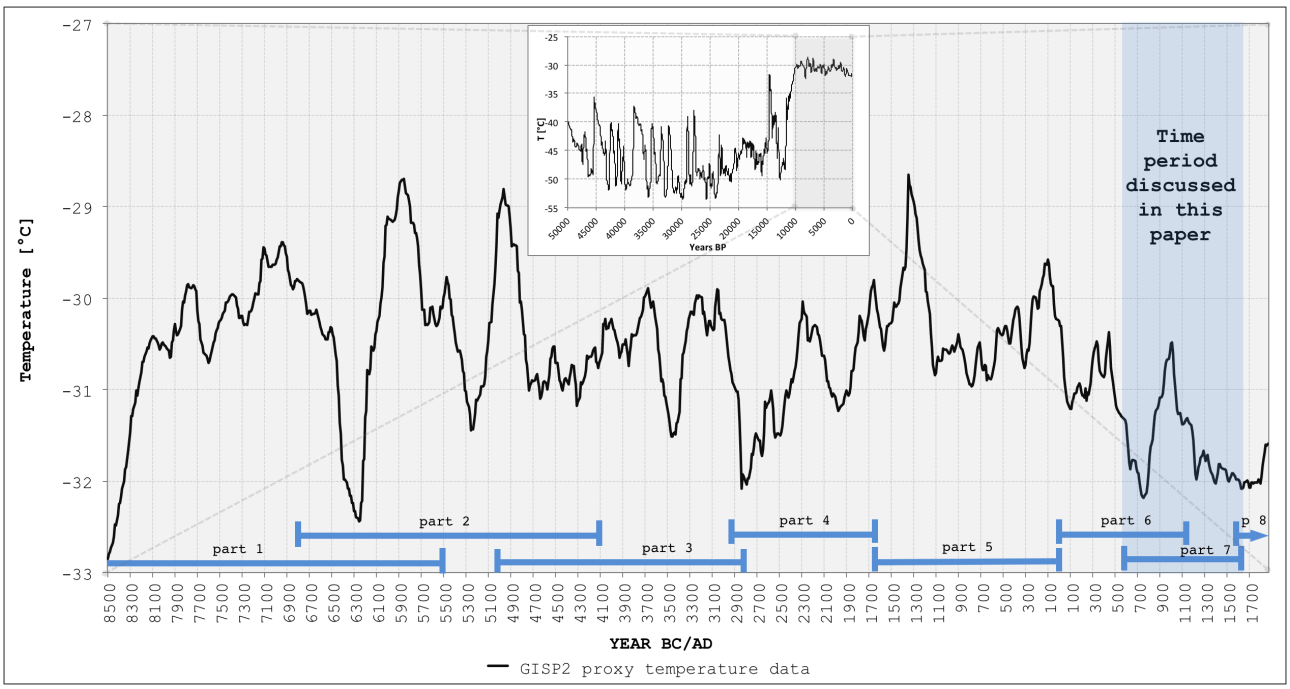

Figure 1. The Holocene GISP2 data (transformed into equidistant time steps) and the period discussed in this paper

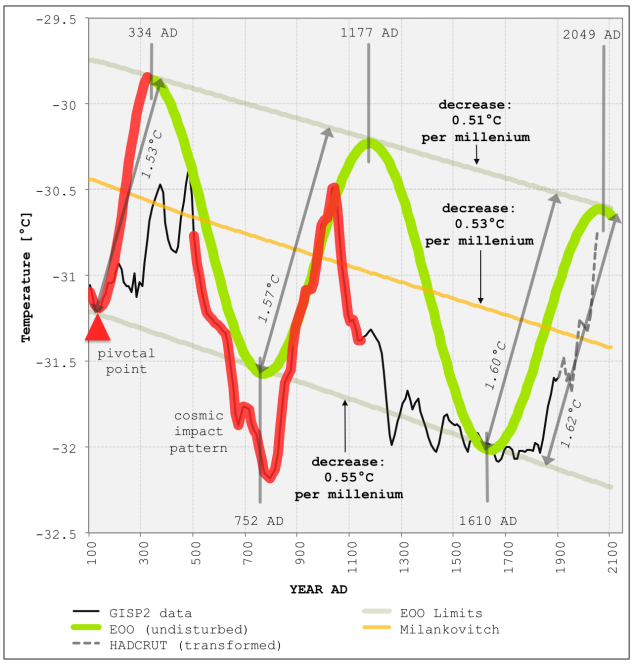

Figure 2. Time span with recognition grid placed

recognition grid is marking all vertical lines for cyclic periodicities.

The very first cycle started in the beginning of the Holocene, at 8108 BC, with a half-wave length of 238 years. The cycles do not show a fixed standard length as all power spectra analyses suggest, but they rather grow in steady increments by 6.93 years per successive half-wave. The actual length today is 439 years. It appears that the possibility of growing cycles never occurred to power spectra analysts. The dates of the cyclic EOO amplitudes for this Holocene paper are: 334 AD (high temperature), 752 AD (low temperature), 1177 AD (high temperature), 1610 AD (low temperature) and 2049 AD (high temperature).

Previous dates are discussed in papers, part 1 to 6. The given high and low temperature amplitudes are connected by sine half-waves. We complete the grid with two horizontally inclined lines, the upper and the lower Earth Orbital Oscillation (EOO) boundary line. The bottom EOO-line constitutes the connecting line between one extraordinary pivotal bottom point at 90 AD and the cycle bottom trough point at 1610 AD. The distance between upper and lower EOO boundary line is the cycle amplitude, which is determined by multiplying the cycle period by the factor of 0.0037. For example, the period 1177 AD to 1610 AD, with 432 years as cycle period #29, produces an EOO amplitude of 1.6°C on the GISP2 borehole temperature scale. This factor is due to the linear relation of the EOO cycle length and EOO cycle amplitude (Seifert, 2010). Earlier, in 7000 BC, in cycle periodicity #5, this distance was 0.98°C for a cycle length of 266 years.

In the center between the two lines runs the Milankovitch line, which since 78 BC has a descent of 0.53°C per millennium on the GISP2 borehole temperature scale. This is the overall climate descent into the coming glacial. The upper EOO boundary line has a descent of 0.51°C/millennium, the lower EOO boundary line a descent of 0.55°C/millennium. Other literature determined 0.31°C/millennium (Esper, 2012) or 0.40°C/millennium (Boell, 2014). Those studies produced lower values, which can be explained by their arbitrary selection of beginning and final dates, which can be either lower or higher, and secondly, they are outside of a long-term Holocene temperature evolution concept. The Milankovitch temperature descent belongs to the general glacial-interglacial temperature evolution, controlled exclusively by the longest solar cycle, the 100,000 year Milankovitch Sun movement cycle. This cycle has no relation to TSI variations and must also not be confounded with an assortment of wiggling, wobbling and turning cycles carried out by the planet Earth itself (varying between 19,000 and 41,000 years - the often quoted precession and obliquity cycles) on which the Milankovitch literature always focusses. All literature on the market, concerning planetary Earth wiggling and turning has no relevance for our Holocene analysis.

2. THE 1ST INTERVAL: 572 AD TO 1050 AD - THE LARGE COSMIC METEOR IMPACT PATTERN

Details of this cosmic meteor impact were given in the previous part 6 of this Holocene series. The Kanmare and Tabban impacts 572/680 AD are described in the literature (Bryant, 2014), (Martos and Abbott, 2006), (Gusiakov and Abbott, 2006). We would like to add some more details, i.e., a comparison of three Holocene cosmic meteor impacts.

This comparison (fig. 3) shows the 5330 BC Macha impact, the 1628 BC EWE-I Atlantic ocean impact and the double Kanmare and Tabban impacts, 572/680 AD. Now, comparing three different Holocene impacts, we observe that the cold spike - hot spike impact pattern feature is identical in dynamics and slopes of temperature evolution and in the development of pointed spikes. Those features are caused by the same forcing mechanics: It is the Cosmic Impact Oscillation (CIO) of the planet Earth, which always takes place when a sizable meteor bolide hits the Earth surface: Every impact that caused Earth oscillation must have a spiky appearance in the GISP2 temperature curve. For explanations of cosmic impact oscillation mechanics, a new paper will be published later in 2017, or see (Seifert and Lemke, 2012).

Figure 3 demonstrates how the two Kanmare-Tabban impacts produced the cold spike of 744 AD followed by

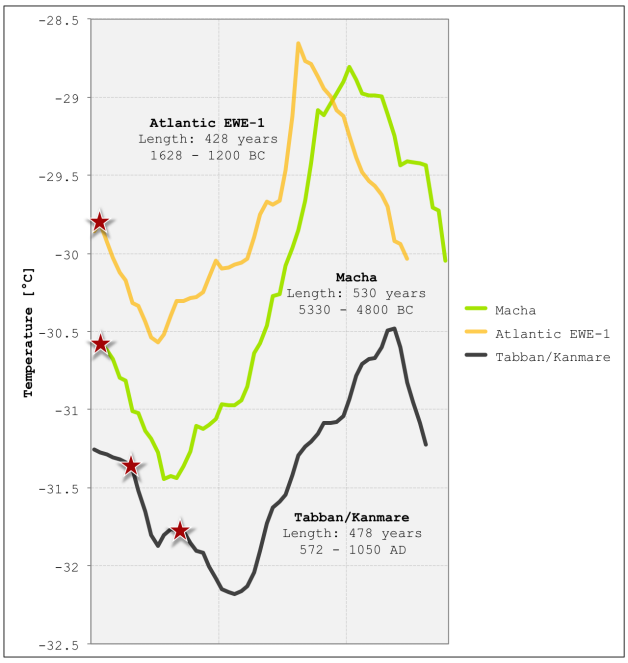

Figure 3. Holocene standard double spike cosmic impact pattern: Comparison of three impacts

the hot spike of 985 AD, from which temperatures again fall until 1050 AD, in order to complete the full double spike pattern. The 985 AD high temperature spike is called Medieval Warm Period (MWP). A major feature of all cosmic impact forcing is that their effects do not remain confined to one region on Earth, but the cold spike - hot spike pattern must be simultaneously present on the entire globe, in the Northern Hemisphere, as in the Tropics, as in the Southern Hemisphere. An ongoing MWP mapping project shows the universal character of the hot spike on Earth (Medieval Warm Period Mapping Project, 2016). Only an external, astronomical impact event, a cosmic meteor impact forcing, is strong enough to produce a simultaneous, cold-hot spike temperature swing all over the globe. No atmospheric or oceanic circulation is capable to achieve this universal cold-hot pattern, but would only move heat from one location to another: A surplus heat in one location would mean a deficit in another location.

In AD 1050, the cosmic impact pattern ends and the second interval of our analysis commences from 1050 AD to 1178 AD.

3. THE 2ND INTERVAL: 1050 AD TO 1178 AD - THE SOLAR INERTIAL MOVEMENT CYCLE (AMO + PDO)

Here we find a fine demonstration of the fifth cosmic climate forcing mechanism, which governs our climate. This fifth mechanism (Seifert and Lemke, 2010) affects the secular climate by periodic small margins visible in the GISP2 time series. We reveal a robust astronomical cycle with a periodicity of exactly 62 years in length (fig. 4). This value of 62 years maintains temperature peaks at constant time intervals for the entire Holocene. Here we show that in a 900 year time period, 300 AD to 1200 AD, the peaks maintain their 62 years periodicity distance. All peak counting started from the AD 2000 base marker peak in backtrack mode over millennia. The astronomical

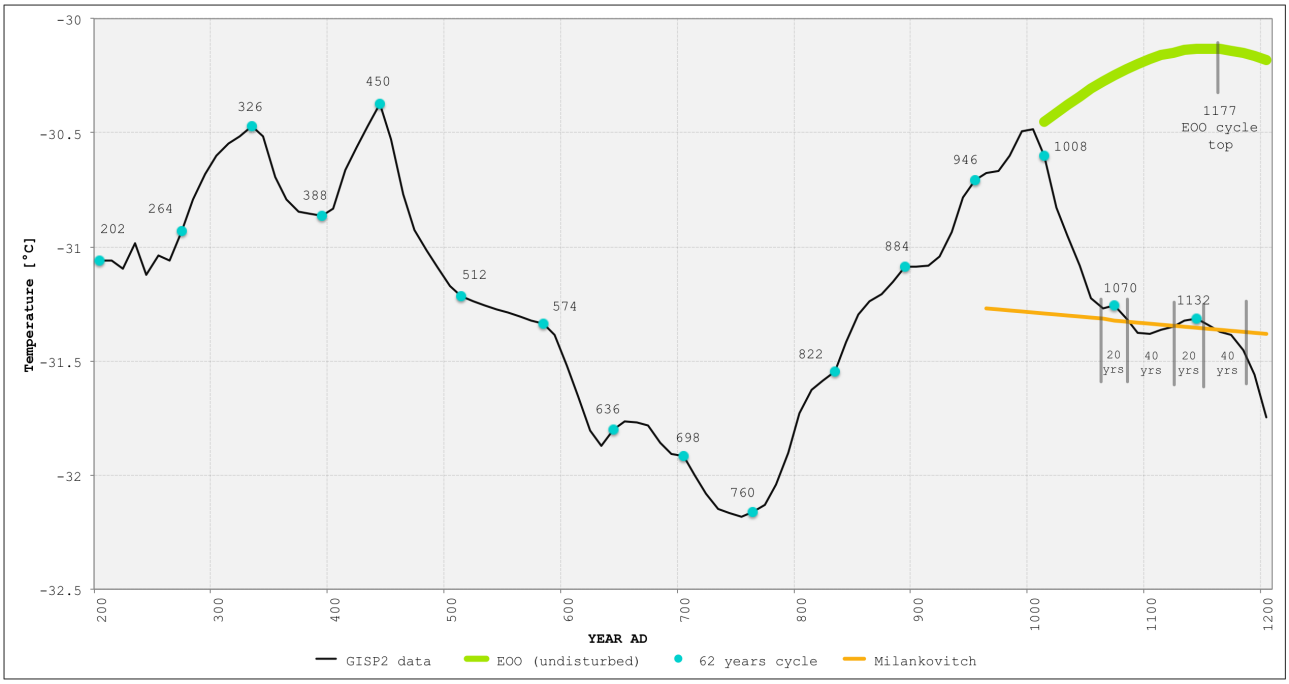

Figure 4. The 62 year cycle

character of this solar SIM cycle is clearly proven and we may quote Stocker (Stocker and Mysak, 1992), that the "internal atmosphere-ocean system is unable to produce a forcing with 'a well defined periodicity'". Thus, the so-called "~60-65 year AMO/PDO-cycle system" is a product of cosmic forcing and is not a cycle with an inherent internal oceanic forcing cause.

We can observe two 62 year periods:

- from 1050 AD, rising to a warm peak at 1071 AD, then subsiding 40 years,
- from 1113 AD, rising to a warm peak at 1133 AD, then subsiding 40 years. At a later time, we will present a separate Holocene 62 year cycle analysis paper based on original, not preprocessed, higher-resolved in time GISP2 measurements, which will show robust 62 year cycle peaks.

Afterwards, the ensuing temperature trend line follows the general Milankovitch decline of 0.53°C/ millennium.

This new temperature trend of the two cycles was suddenly interrupted in 1178 AD, when the next cosmic meteor impact occurred.

4. THE 3RD INTERVAL: 1178 AD TO 1590 AD - THE LUNAR IMPACT AND ORBITAL STABILIZATION PERIOD

The demonstration in figure 5 explains this unusual period.

We observe: The cosmic meteor impact strike sent global temperatures straight down into the cold spike, from 1178 to 1207 AD. The large distance between individual GISP2 measurement points after 1178 AD to 1207 AD demonstrates clearly the event abruptness. This event was the June 1178 meteor impact on the Moon, which was witnessed by 5 monks in Canterbury, England. They reported a strong shaking of the Moon, followed by fire columns arising out from the Moon´s rim into a considerable distance into space, which was followed by darkening of the lunar light by impact plume dust (The 1178 AD Canterbury event, 2016). It was speculated that the lunar Giordano Bruno crater was the cosmic impact location. This, however, is unlikely because the impact fire column went into space and not towards Earth, which certainly would have happened, if the Moon's face were impacted. The impact crater therefore, must be located on the sides of the Moon, which are showing into space and can be observed from earth. We confirm this event with certainty, pointing to the rapid temperature drop and the developing CIO cold spike. A second proof is the extent of the temperature drop to below the lower EOO boundary line, which can solely occur after preceding cosmic meteor impacts (see figure 5, the red triangular low spikes).

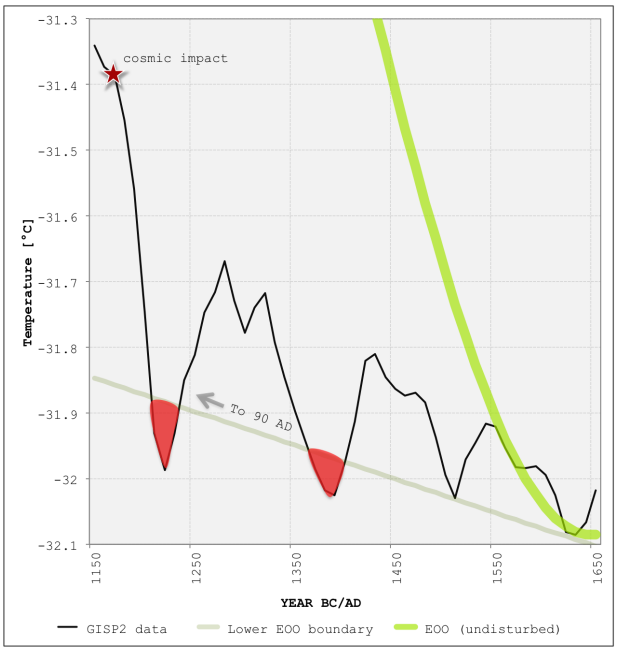

Figure 5. Effects of the lunar impact in 1178 AD and the orbital stabilization period of the Earth

Concerning the drawing of the lower EOO boundary line: It is a straight line from the pivotal low of -31.224°C in 90 AD to the bottom EOO peak in 1610 AD with -32.07°C. The line also touches the -32.02°C point at 1495 AD and has a millennial descent of 0.55°C, obtained by comparing the two 90 AD and 1610 AD temperatures.

As temperatures rose out of the cold spike of 1207 AD, a very interesting, very rare event set in: A spiral movement of the Earth-Moon gravitational barycenter around the regular Earth orbit line as shown in figure 6.

The explanation: Moon and Earth form a joint gravitational unit in its course around the Sun. Both, Moon and Earth have a common "Earth-Moon Barycenter" on the ecliptic orbital plane. Now the impact event occurred: The Moon was severely hit and was pushed into the 3-D space Z-dimension (to above - in spring - and to below - in autumn - of the ecliptic plane). This Z-dimension is ruled by only small Sun and Earth gravitational forces. The impact event dragged both the barycenter and Earth out of the ecliptic plane, but only a certain distance into this Z-dimension at both ends of the minor axis, leaving the major axis - from Perihelion to Aphelion - unchanged. In order to regress to the initial position, the Earth-Moon barycenter carried out four shrinking spiral loops to approach and occupy again the regular barycenter orbit around the Sun. We can see the following:

1. A trend line
2. The declining maximum spiral temperature line
3. Regular angles of temp increases/decreases for the four spiral rotations.

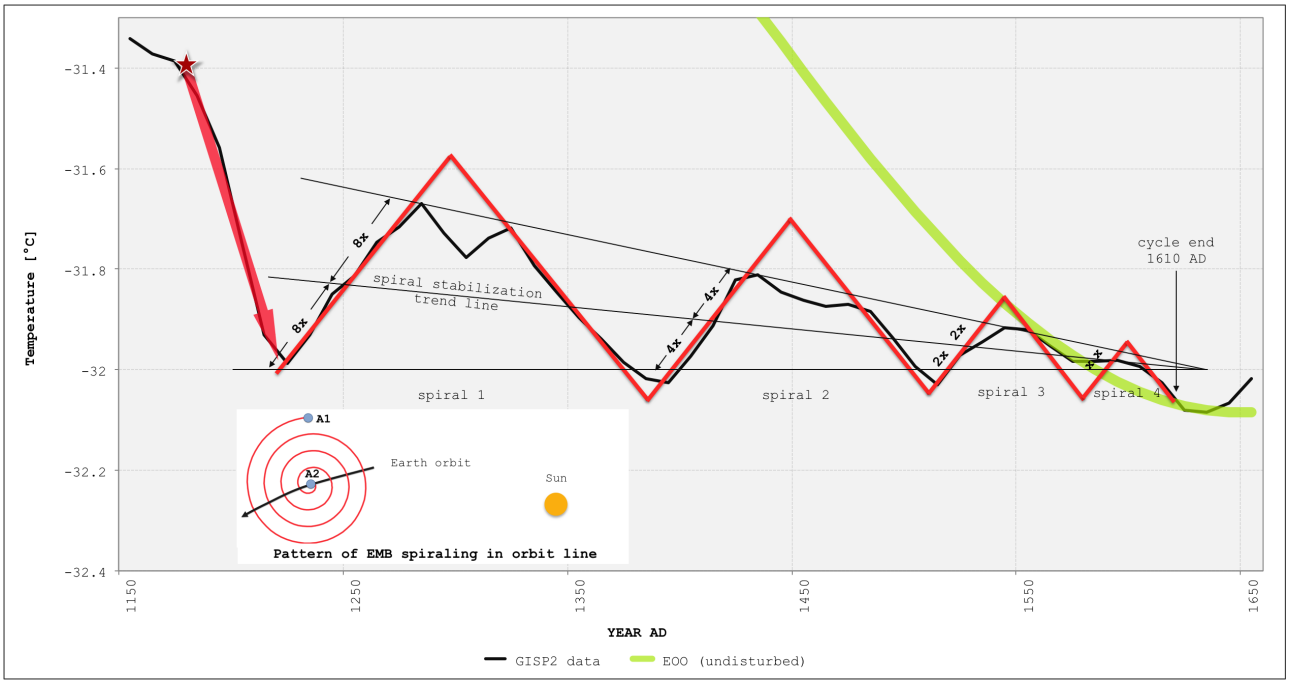

Figure 6. Spiral movement of the Earth-Moon Barycenter

4. A regular oscillation decrease in the relation 8 : 4 : 2 : 1

The 4th spiral rotation completed in 1610 AD, when the next pattern, the EOO-LIA-trough bottom started.

An additional indication for this spiral rotation movement is the failure of the sequence of five 62 year SIM peaks to clearly appear (1256 AD, 1318 AD, 1443 AD, 1504 AD and 1566 AD). Three peak dates are not visible; and two peak dates, 1443 AD and 1504 AD, appear solely as two mini "pimples", as cycle residues, but visible by enlarging the temperature graph. Such a long signal failure sequence did not occur in previous Holocene millennia. The explanation is that the EMB spiral rotation forces overwhelmed and cancelled out the 62 year cycle peak effects in GISP2.

To the role of volcano mega-eruptions: There are two of them, 1257 AD and 1458 AD, within this time span. General short-lived volcano cooling to a maximum of 10 years was proven by (Sigl and Winstrup, 2015). For both eruption dates, no global cooling is observed. Another interesting point is that within this EMB-stabilization period, two cold decades exist, the Dantean Anomaly - "The Great Famine" (1310-1321 AD) and the 1430s Minimum (1430-39 AD). Both occur, visible in the temperature graph, as a decline period after a temperature high. This phenomenon can be explained with orbital stabilization, which produces decades of hot and cold climates. The 1430s period was recently studied by Camenisch and 32 other modelers (Camenisch, 2016), but, quote: "Comprehensive climate models indicate that these [cold] conditions occurred only by chance due to the chaotic internal variability of the climate […] External forcing [...] cannot explain [model] reconstructions". This study insist on "chaotic variability", where there is none. Instead, there is a clear regularity in external forcing, as shown in figures 5 and 6. The Camenisch paper serves as fine example for the value of modeling and simulation: The Climate Pattern Recognition method easily identified the orbital stabilization pattern. A last point: Somewhere, not clearly defined, around 1460 AD, a solar sunspot minimum, the "Spoerer Minimum" was reconstructed. However, we cannot observe a temperature lowering effect of this Minimum in GISP2, as has been claimed. Rather, temperatures in Spoerer times move within the spiral loop stabilization frame, both up and down, and missing sunspot temperature lowering on Earth cannot be observed.

5. THE 4TH INTERVAL: 1590 AD TO 1640 AD - THE EOO - LIA BOTTOM TROUGH PATTERN

Figure 6 shows the EOO cycle bottom at the right hand side as a low peak from 1610-1630 AD. The vertical line for the EOO periodicity date is at 1610 AD. There, five other lines unite: The descending EOO-sine line from its peak in 1177 AD; second, the GISP2 measurement data line; third, the maximum spiral temperature line; fourth, the spiral stabilization trend line; and fifth, the EMB spiral bottom peak line. The bottom trough lasts about 50 years, from 1590 to 1640 AD; minimum temperature is -32.08°C on the GISP2 borehole scale. We use this temperature trough as a base marker point for determining the millennial Milankovitch line descent since 78 BC:

Twenty nine periodicities exist between 8108 BC and 1610 AD. The factor of 0.0037 period lengths converts period lengths into their respective amplitudes. We are thus able to determine for each single year EOO periodicity and amplitude by interpolation. For the pivotal date of 90 AD, within cycle period #26, the lower EOO boundary line, according to GISP2, is positioned at -31.224°C. This relates to an upper EOO boundary point at -29.69°C and a Milankovitch line point of -30.46°C, running in the center.

For the LIA bottom trough line at 1610 AD, of cycle period #29, the lower EOO boundary line according to GISP2 lies at -32.08°C. This relates to an upper EOO boundary line point at about -30.50°C and a Milankovitch line point in the center at about -31.30°C. By comparing those 3 temperature values of 90 AD, to the corresponding 3 values at the date 1610 AD, we obtain a millennial temperature descent (into the coming glacial) of the central Milankovitch line of 0.53°C. The descent of the upper EOO line is slightly less, 0.51°C, and of the lower EOO line slightly more, 0.55°C , because the EOO amplitude increases over time. In the next paper, Holocene part 8, we will compare the 3 periodicity temperatures of the 1610 AD bottom trough to those of the alternating future high peak of 2049 AD.

6. CONCLUSIONS

The Climate Pattern Recognition analysis achieved a clear identification of four different climate pattern periods in this given time span. It should also be mentioned that, on the other hand, computer simulating and modeling for 30 years was not competent to identify even one single of all four presented periods. The performance of our analysis identified many other climate pattern periods, which we identified for the past 10,000 years. Cosmic climate forcing mechanisms, five in existence, govern the entire Holocene.

We will enumerate those climate forcing mechanisms again: Three are of solar motion origin, one is produced by oscillations of the Earth orbit and the last is the result of cosmic meteor impacts in the Earth-Moon system. The mechanisms are:

1. The 100,000 year Milankovitch solar motion cycle, which, at present, produces a 0.53°C temperature descent per millennium towards the next glacial,
2. The 62 year SIM solar barycenter motion cycle, which aggregates robust and regular small-scale peaks to the secular temperature evolution,
3. The SMA - solar motion anomaly, which this time is absent within this particular time span,
4. The Earth Orbital Oscillation, which produces growing cycles of alternating cold and warm periods, starting out from 8108 BC, with an initial 238 years in length, as the 1st cycle period. The 29th (cold) cycle bottom peak is in 1610 AD; the 30th (warm) cycle top peak is scheduled for 2049 AD,
5. The last forcing mechanism is the CIO, the cosmic meteor impact oscillation mechanism, which necessarily produces a distinct double spike temperature swing pattern in GISP2: The first half, a cold spike, followed by the second half, the rebound hot spike. Holocene examples are demonstrated. The following paper, part 8, will deal with the time span 1600 AD to 2050 AD; An additional part 9 will forecast the remaining time to the Holocene end.

REFERENCES

Alley, R.B.: The Younger Dryas cold interval as viewed from central Greenland, Quaternary Science Reviews, Volume 19, Issues 1-5, 2000, http://www.ncdc.noaa.gov/paleo/icecore/greenland/greenland.html,

Alley, R.B.: GISP2 Ice Core Temperature and Accumulation Data. IGBP Pages/World Data Center for Paleoclimatology, Data ContributionSeries #2004-013, NOAA/NGDC Paleoclimatology Programs, Boulder, CO, USA

Boell, A. et.al.: Late Holocene primary productivity and sea surface temperature variations in the northeastern Arabian Sea: Implications for winter monsoon variability, Paleoceanography, 29, 778-794, doi: 10.1002/2013PA002579, AGU Publications 2014

Bryant, E.: Tsunami, the Underrated Hazard, Book, Third edition 2014, Springer publishers, ISBN 978-3-319-06132-0, doi: 10.1007/978-3-319-06133-7

Camenisch, C. et. al.: The 1430s: a cold period of extraordinary climate variability during the earlier Spoerer minimum with social and economic impacts in north-western and central Europe, Clim. Past, 12, 2107-2016, doi: 10.5194/cp-12-2107-2016,2016

Esper, J.; et al.: Orbital foring of tree-ring data, Nature Climate Change (2012), doi: 10.1038/nclimate 1589 http://www.geo.uni-mainz.de/Dateien/Esper_2012_NatureCC.pdf and http://www.nature.com/nclimate/journal/vaop/ncurrent/full/nclimate1589.html

Gusiakov, V.; Abbott, D.H.; Bryant, E.A.; Masse, W.B.: Megatsunamis of the world oceans: chevron dune formation, micro-ejecta and rapid climate change as the evidence of recent bolide impacts (2010), in: T.Beer (ed.) Geophysical Hazards, Springer Scienc and Business Media B.V., doi: 10.1007/978-90-481-3236-2_13

http://academiccommons.columbia.edu/download/fedora_content/download/ac:193311/CONTENT/Gusiakovetal_2009_Tsunami_Chevrons.pdf

Martos, S.; Abbott, D.H.: Impact spherules from the craters Kanmare and Tabban in the Gulf of Carpentaria, in: The Geological Society of America (GSA), the 2006 Philadelphia Annual Meeting, 22-25 Oct 2006, paper 118-119

Medieval Warm Period Mapping Project, 2016, http://kaltesonne.de/mapping-the-medieval-warm-period/ and http://t1p.de/mwp

Seifert, J.: Das Ende der globalen Erwärmung, Berechnung des Klimawandels, (2010), 109 pp., Pro Business Verlag Berlin, ISBN 978-3-86805-604-4, http://www.amazon.de/Das-Ende-globalen-Erwärmung-Klimawandels/dp/3868056041

Seifert, J., Lemke, F.: Five climate forcing mechanisms govern 20,000 years of climate change, 2012, http://www.knowledgeminer.eu/climate_papers.html

Sigl, M.; Winstrup, M. et. al: Timing and climate forcing of volcanic eruptions for the past 2,500 years, Nature 523, 543-549 (30 July 2015) doi:10.1038/nature14565

Stocker, T.F.; Mysak, L.A.: Climatic fluctuations of the century time scale: A review of high-resolution proxy data and possible mechanisms, Climate Change 20, p. 227-250, March 1992, Kluver Academic Publishers, N.L. http://www.climate.unibe.ch/~stocker/papers/stocker92cc.pdf

The 1178 AD Canterbury event, 2016, https://en.wikipedia.org/wiki/Giordano_Bruno_(crater)